COMPUTATIONAL MODELING OF INTERNAL COMBUSTION ENGINES

Nelson Prado Rodrigues Cró
Janito Vaqueiro Ferreira
Waldyr Luiz Ribeiro Gallo
Marcelo Gennari Tanikawa
University of Campinas – Campinas - SP - Brazil
nelson_cro@hotmail.com
janito@fem.unicamp.br
gallo@fem.unicamp.br
marcelo.tanikawa@gmail.com

Abstract. This paper describes the development of a computational simulation model for internal combustion engines with spark ignition, powered by ethanol fuel which includes the combustion with finite duration, the instantaneous heat transfer and the intake and exhaust processes. The simulation model calculates the thermodynamic properties of each element involved in the process at every discretized instant of the engine cycle using as input the data related to the engine and to its intended operating regime. The simulation model has as a result the instantaneous temperature and instantaneous pressure profiles inside of the cylinder as a function of the crankshaft angle in the range of one cycle.

Keywords: engine, computational simulation, combustion, spark ignition, ethanol fuel

1. INTRODUCTION

The computational simulation models are of great importance in the development and in the optimization of engines, as they allow a significant reduction in time and in resources invested in testing, which makes them increasingly an important tool for companies, universities and institutes research worldwide.

In this way, this article presents an algorithm robust and sufficiently developed to generate estimates of the pressure and temperature profiles of real internal combustion engines and to assist in efficient conduction of the engine tests.

2. COMPUTATIONAL SIMULATION MODEL

The developed computational simulation model seeks to reproduce the thermodynamic cycle of internal combustion engines with spark ignition, powered by ethanol fuel using as input the data related to the engine and to its intended operating regime. From the input data (Tab. 3), the algorithm performs preliminary calculations to the simulation, mainly related to the engine geometry equations (section 2.1.1.) and to the balancing combustion reaction (section 2.1.2.). Then, the algorithm develops the simulation respecting a thermodynamic model (section 2.2.) which distinguishes between the open phase (section 2.2.1.) and the closed phase (section 2.2.2.) of the engine cycle and takes into consideration the ideal gas model (section 2.1.3.) to calculate the properties of the substances (section 2.1.4.), the intake and exhaust processes (section 2.1.5.), the phenomena of the instantaneous heat transfer with the cylinder walls (section 2.1.6.) and the combustion process with finite duration (section 2.1.7.). After the simulation achieved the convergence, the algorithm prints the temperature and pressure profiles as a function of the crankshaft angle and the instantaneous pressure profile as a function of instantaneous volume.

2.1. Theoretical Fundamentals

The main formulations used in the modeling of the algorithm are described below.

2.1.1. Engine Geometry Equations

The geometry of a conventional engine is shown in Fig. 1. The instantaneous displacement $D(\theta)$, the bore d, the piston stroke L, the length of the connecting rod l, the radius R and angle θ of the crankshaft, the connecting rod angle φ and the shape of combustion chamber, which was admitted cylindrical, are represented in Fig. 1.

The used thermodynamic model requires information concerning the geometric parameters of the engine to be simulated. Among these can be mentioned the shape of the combustion chamber, the compression ratio TC, the bore d, the piston stroke L and the length of the connecting rod l. After defining these parameters, it is possible to calculate the instantaneous piston displacement $D(\theta)$, the instantaneous heat transfer area $A(\theta)$, the instantaneous volume $V(\theta)$ and the engine displacement V_c, which are presented respectively by Eq. (1), Eq. (2), Eq. (3) and Eq. (4).

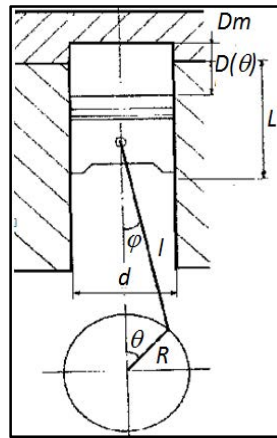Figure 1 - Geometry of a conventional engine (Gallo, 1990).

$$D(\theta) = \frac{L}{2} * (1 - cos\,\theta) + l * \left(1 - cos\,\varphi(\theta)\right) \tag{1}$$

$$A(\theta) = (D(\theta) + D_m) * \pi * d + 2 * A_p \tag{2}$$

$$V(\theta) = (D(\theta) + D_m) * A_p \tag{3}$$

$$V_c = A_p * L \tag{4}$$

, where the connecting rod angle $\varphi(\theta)$, the piston area A_p and the length of the combustion chamber D_m are represented respectively by Eq. (5), Eq. (6) and Eq. (7)

$$\varphi(\theta) = \sin^{-1}\left(\frac{L}{2*l} * \sin\theta\right) \tag{5}$$

$$A_p = \frac{\pi * d^2}{4} \tag{6}$$

$$D_m = \frac{L}{(TC-1)} \tag{7}$$

The calculation related to the gas flow through the intake and exhaust valves requires knowledge of the engine project parameters. These are the nominal diameter of intake d_{va} and exhaust d_{ve} valves, the camshaft geometry and the gas flow area through the intake A_{va} and exhaust A_{ve} valves.

According to Sherman and Blumberg (1977), the hypothesis of parabolic shape of valve lift is very close to the real engines and simpler to treat analytically. This model shows that the valve lift is composed by concordance of three parabolas, as shown in Fig. 2. It is defined the coefficient YD_v as a form to make the value of valve lift dimensionless. The coefficient YD_v is the ratio between the valve lift and its nominal diameter, as presented by Eq. (8).
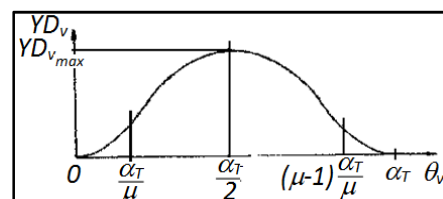
$$YD_v = \frac{e_v}{d_v} \tag{8}$$

Figure 2 – Dimensionless profile of valve lift (Gallo, 1990).

Thus, the equations to valve lift as a function of angular displacement to valve opening α is given by Eq. (9), Eq. (10) and Eq. (11).

$$YD_v = a_1 * \alpha^2 + b_1 * \alpha + c_1 \qquad\qquad 0 \leq \alpha \leq \frac{\alpha_T}{\mu} \tag{9}$$

$$YD_v = a_2 * \alpha^2 + b_2 * \alpha + c_2 \qquad\qquad \frac{\alpha_T}{\mu} \leq \alpha \leq (\mu - 1) * \frac{\alpha_T}{\mu} \tag{10}$$

$$YD_v = a_3 * \alpha^2 + b_3 * \alpha + c_3 \qquad\qquad (\mu - 1) * \frac{\alpha_T}{\mu} \leq \alpha \leq \alpha_T \tag{11}$$

Applying the boundary conditions in Eq. (9), Eq. (10) and Eq. (11), it is obtained the parameters given by Eq. (12), Eq. (13), Eq. (14) and Eq. (15)

$$a_1 = \frac{4*YD_{max}*(1-r)}{\alpha_T{}^2} \qquad\qquad b_1 = 0 \qquad\qquad c_1 = 0 \tag{12}$$

$$a_2 = \frac{a_1}{r} \qquad\qquad b_2 = -a_1 * \frac{\alpha_T}{r} \qquad\qquad c_2 = a_1 * \alpha_T{}^2 * \left[\frac{1}{4*r*(1-r)} \right] \tag{13}$$

$$a_3 = a_1 \qquad\qquad b_3 = -2 * a_1 * \alpha_T \qquad\qquad c_3 = a_1 * \alpha_T{}^2 \tag{14}$$

$$\mu = 2 * (1 - r) \tag{15}$$

, where r is admitted with value 4 and $YD_{máx}$ with value 0,3.

The typical geometry of poppet valve head and its seat are shown in Fig. 3, in which the dimensions are a function of the valve diameter d_v.
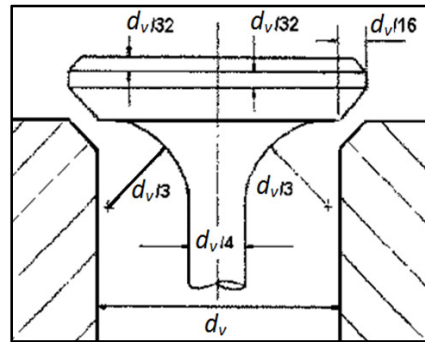

Figure 3 – The typical geometry of poppet valve head and its seat (Gallo, 1990).

According to Gallo (1990), the flow area through the valves is variable and it is defined on the perpendicular direction to the flow. Thus, it is identified three distinct flow regimes, which are characterized by the minimum distance between the valve and its seat, in accordance with Eq. (16), Eq. (17) and Eq. (18).

$$A_v = \pi * e_v * \frac{\sqrt{2}}{2} * \left(d_v + \frac{e_v}{2} \right) \qquad\qquad 0 < YD_v \leq 0.125 \tag{16}$$

$$A_v = \frac{17*\pi*d_v}{16} * \sqrt{e_v{}^2 - \frac{e_v*d_v}{8} + \frac{d_v{}^2}{128}} \qquad\qquad 0.125 < YD_v \leq 0.274 \tag{17}$$

$$A_v = \frac{15*\pi*d_v{}^2}{64} \qquad\qquad 0.274 < YD_v \leq YD_{máx} \tag{18}$$
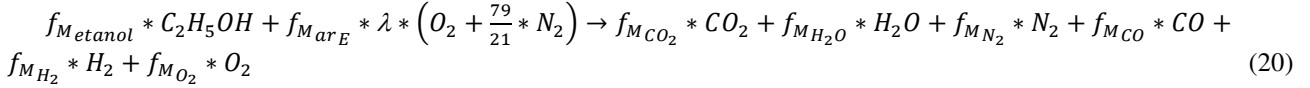
2.1.2. Balancing Combustion Reaction

In this paper, it is assumed that the working fluid consists of anhydrous ethanol C_2H_5OH, of air, of carbon dioxide CO_2, of water H_2O, of nitrogen N_2, of carbon monoxide CO, of hydrogen H_2 and of oxygen O_2, whose fraction amounts depend on the process step. The molar composition of air is assumed to be 21% oxygen O_2 and 79% nitrogen N_2 and the air/fuel mixture is admitted homogeneous.

The mixture admitted to the spark ignition engines is a mixture of air and fuel, which could be a stoichiometric, a rich or a lean mixture. The stoichiometric air/fuel mixture ($\lambda=1$) is one in which the theoretical reagent amounts produce a complete combustion reaction, while the rich mixture ($\lambda<1$) has shortage of air and the lean mixture ($\lambda>1$) has excess of air. The relationship between the actual air/fuel ratio r_{ac} and the stoichiometric air/fuel ratio r_{acE} define the stoichiometric ratio λ, which is shown in Eq. (19).

$$\lambda = \frac{r_{ac}}{r_{acE}} \tag{19}$$

The complete combustion never occurs in practice due to inefficiencies in the process as the flame quenching near the cylinder walls, the crevices and the absence of oxidizing elements, which result is an unburned fuel portion. In addition, some fuel molecules do not burn completely during the combustion process.

In this article, it is assumed complete combustion in the process equations however it is applied a coefficient called "combustion efficiency" η_c, proposed by Alla (2002), for taking into account the process inefficiencies and also the thermal dissociation effects, which occur in real combustion process. Thus, it is presented in Eq. (20) the balancing combustion reaction, where f_M is the molar fraction of each one of the involved substances.

$$f_{M_{etanol}} * C_2H_5OH + f_{M_{ar_E}} * \lambda * \left(O_2 + \frac{79}{21} * N_2\right) \rightarrow f_{M_{CO_2}} * CO_2 + f_{M_{H_2O}} * H_2O + f_{M_{N_2}} * N_2 + f_{M_{CO}} * CO + f_{M_{H_2}} * H_2 + f_{M_{O_2}} * O_2 \tag{20}$$

The balancing of Eq. (20) for the stoichiometric air/fuel mixture implies formation of carbon dioxide CO_2, of water vapor H_2O and of nitrogen N_2 as resulting gases from the complete combustion. In the rich mixtures it is also formed hydrogen H_2 and carbon monoxide CO while in the lean mixtures there is excess of oxygen O_2 in the exhaust gas.

2.1.3. Ideal Gas Model

The assumption of ideal gas is valid under the conditions studied in this article since, where according to Zacharias (1967), for pressures up to 100 atm and temperatures up to 2500 K the compressibility factor is equal to 1.

2.1.4. Calculation of the Thermodynamic Properties of Substances

From the values of specific heat at constant pressure c_p found in JANAF Thermodynamic Tables, which were developed by Stull and Prophet (1971), the polynomials given in Eq. (21) and Eq. (22) are obtained. These polynomials predict the specific heat at constant pressure c_p for each one of the "s" substances involved in the process on the basis of the temperature, which is obtained by least square.

$$c_{p_s}(T) = \sum_{n=0}^{n=6}(D_{n_s} * T^n) \qquad 300\ K < T \leq 1500\ K \tag{21}$$

$$c_{p_s}(T) = \sum_{n=0}^{n=6}(E_{n_s} * T^n) \qquad 1500\ K < T \leq 6000\ K \tag{22}$$

In the same way, from thermodynamic tables found in Raznjevic (1970), it is obtained the polynomial to predict the specific heat at constant pressure for anhydrous ethanol, which is presented in Eq. (23)

$$c_{p_{C2H5OH}}(T) = \sum_{n=0}^{n=6}(C_n * T^n) \qquad 273\ K < T \leq 1473\ K \tag{23}$$

The polynomial constants C_n, D_n and E_n are shown respectively in Tab. 1.

Table 1 – Polynomial constants C_n, D_n and E_n.

J/mol/K	C_0	C_1	C_2	C_3	C_4	C_5	C_6	error
C_2H_5OH	3,93519E+01	4,33807E-02	4,40343E-04	-8,75965E-07	7,84528E-10	-3,48376E-13	6,16882E-17	0,044

J/mol/K	D_0	D_1	D_2	D_3	D_4	D_5	D_6	error
CO_2	1,65169E+01	1,00510E-01	-1,40038E-04	1,42122E-07	-9,49168E-11	3,58207E-14	-5,70443E-18	0,006
H_2O	3,63690E+01	-3,17661E-02	1,12809E-04	-1,60029E-07	1,30177E-10	-5,60955E-14	9,79774E-18	0,006
N_2	2,97830E+01	1,57533E-03	-1,66246E-05	6,96896E-08	-8,21238E-11	4,12997E-14	-7,74701E-18	0,007
CO	3,10961E+01	-1,37896E-02	2,40220E-05	9,87346E-09	-3,69665E-11	2,40428E-14	-5,09193E-18	0,008
H_2	2,24823E+01	4,80380E-02	-1,35912E-04	1,94249E-07	-1,47045E-10	5,76529E-14	-9,25454E-18	0,011
O_2	3,41723E+01	-5,11033E-02	1,78999E-04	-2,57887E-07	1,93779E-10	-7,48794E-14	1,17867E-17	0,003

J/mol/K	E_0	E_1	E_2	E_3	E_4	E_5	E_6	error
CO_2	3,43457E+01	3,47153E-02	-1,96667E-05	6,28815E-09	-1,14621E-12	1,11257E-16	-4,44867E-21	0,015
H_2O	1,57704E+01	3,71696E-02	-1,55679E-05	3,92132E-09	-5,93371E-13	4,95065E-17	-1,73018E-21	0,013
N_2	2,28490E+01	1,63085E-02	-8,43104E-06	2,47165E-09	-4,15904E-13	3,74694E-17	-1,39608E-21	0,004
CO	2,37854E+01	1,57972E-02	-8,35981E-06	2,49778E-09	-4,26617E-13	3,89644E-17	-1,47549E-21	0,009
H_2	2,44633E+01	4,65448E+02	1,87247E-06	-1,48702E-09	3,91309E-13	-4,62159E-17	2,04913E-21	0,005
O_2	3,17898E+01	4,97753E-03	-2,38051E-06	1,17155E-09	-3,12398E-13	3,94659E-17	-1,85715E-21	0,007

Drawing on the ideal gas model, it is obtained the specific enthalpy h_s by Eq. (24) and the specific internal energy u_s by Eq. (25) for each substance

$$h_s = h_{f_s} + \int c_{p_s} dT \tag{24}$$

$$u_s = h_s - R * T \tag{25}$$

, where h_{fs} is the formation enthalpy and R de the universal gas constant.

Although the polynomial to predict the specific heat at constant pressure of the anhydrous ethanol has been obtained for values of temperature between 273 K and 1473 K, the present study used the relationship to higher temperatures. It was verified that the extrapolation of values is consistent and the errors related to this extrapolation weren't significant in the results, since the calculation is based on the variation of the property amounts and not on its absolute values.

2.1.5. Instantaneous Heat Transfer with the Walls

According to Gallo (1990), in the global models of instantaneous heat transfer in the engines, a quasi-permanent regime is assumed, which validates the rate of heat transfer expression with the cylinder walls δQ_p given by Eq. (26).

$$\delta Q_p = h_p(\theta) * A(\theta) * \left[T(\theta) - T_p\right] * \left(\frac{60}{2*\pi*N}\right) * d\theta \tag{26}$$

Thus, it is defined δQ_p as a function of instantaneous area $A(\theta)$, of cylinder wall temperature T_p, of instantaneous gas temperature $T(\theta)$, of heat transfer coefficients $h_p(\theta)$ and of engine speed N.

Many relationships to obtain the heat transfer coefficients were found in the literature. However, the choice of these coefficients was based on the comparative study correlations performed by Gallo (1990). Thus, the correlation proposed by Hohenberg (1979) was considered the most convenient for the closed phase and it is given by Eq. (27).

$$h_p(\theta) = F_1 * V(\theta)^{-0,06} * P(\theta)^{0,8} * T(\theta)^{-0,4} * \left(V_p + F_2\right)^{0,8} \tag{27}$$

The most suitable correlations to the heat transfer coefficient for the open phase of the engine cycle were proposed by Nishiwaki (1979), which are given in Eq. (28) for the intake process and in Eq. (29) for the exhaust process

$$h_p(\theta) = F_3 * D(\theta)^{-0.193} * \left(V_p * P(\theta)\right)^{0,807} * T(\theta)^{-0,534} \tag{28}$$

$$h_p(\theta) = F_4 * D(\theta)^{-0.422} * \left(V_p * P(\theta)\right)^{0,578} * T(\theta)^{-0,199} \tag{29}$$

, where V_p is the mean piston speed and F_1, F_2, F_3 and F_4 are adjustable constants for each engine, but have as usual values 130, 1,4, 82,3 and 679 respectively.

2.1.6. Combustion Process with Finite Duration

Regarding the combustion with finite duration, among the burning fuel models found in the literature, it was chosen the Wiebe model because since its development in 1967, it has been the most frequently used model in research on thermodynamic combustion modeling. The Wiebe function, which determines the mass fraction burned of fuel, is given by Eq. (30)

$$X_w(\theta) = 1 - exp\left[-a * \left(\frac{\theta - \theta_i}{\Delta\theta_c}\right)^{m+1}\right] \tag{30}$$

, where θ_i is the start angle of combustion, $\Delta\theta_c$ is the angular duration of the combustion process and a and m are adjustable parameters for each engine. Varying the parameters a and m, it is observed a significant modification of the shape curve. According to Heywood (1988), the usual values to the parameters a and m are 5 and 2 respectively.

2.1.7. Intake and Exhaust Processes

It was applied the model found in Gallo (1990) for the gas mass flow through the valves, in which it is assumed a quasi-permanent process with the isentropic flow hypothesis modified by a discharge coefficient C_d, which is defined by Eq. (31).

$$C_d = \frac{\dot{m}}{\dot{m}_{isent.}} \tag{31}$$

Furthermore, the determination of a gas mass flowing through the valve in the case of subsonic and sonic flow is obtained by Eq. (32) and Eq. (33) respectively

$$dm = \left[\frac{C_d(\theta)*A_v(\theta)*P_y}{\sqrt{R_-*T_y}}\right] * \sqrt{\left(\frac{2*\gamma}{\gamma-1}\right)*\left[\left(\frac{P_x}{P_y}\right)^{\frac{2}{\gamma}} - \left(\frac{P_x}{P_y}\right)^{\frac{\gamma+1}{\gamma}}\right]} * \left(\frac{60}{2*\pi*N}\right)*d\theta \qquad \frac{P_x}{P_y} < \left(\frac{2}{\gamma+1}\right)^{\frac{\gamma}{\gamma-1}} \qquad (32)$$

$$dm = \left[\frac{C_d(\theta)*A_v(\theta)*P_y}{\sqrt{R_-*T_y}}\right] * \sqrt{\gamma*\left(\frac{2}{\gamma+1}\right)^{\frac{\gamma+1}{2*(\gamma-1)}} * \left(\frac{60}{2*\pi*N}\right)*d\theta} \qquad \frac{P_x}{P_y} \geq \left(\frac{2}{\gamma+1}\right)^{\frac{\gamma}{\gamma-1}} \qquad (33)$$

, where P_x and P_y are the pressures upstream and downstream of the flow, respectively, and γ is the ratio between the specific heats given by Eq. (34).

$$\gamma = \frac{c_p}{c_v} \qquad (34)$$

The discharge coefficient C_d followed the methodology adopted by Kastner *et al.* (1963) in which, based on tests with the different pressure ratios and valve diameters, it was obtained a single curve to the discharge coefficient as a function of dimensionless coefficient YD_v. The relationship for C_d is given by Eq. (35)

$$C_d(YD_v) = \sum_{n=0}^{n=10}(B_n * YD_v{}^n) \qquad 1500\,K < T \leq 6000\,K \qquad (35)$$

, where the polynomial constants B_n are shown in Tab. 2.

Table 2 – Polynomial constants B_n to discharge coefficient C_d.

B_0	B_1	B_2	B_3	B_4	B_5	B_6	B_7	B_8	B_9	B_{10}
9,99988E-01	7,63357E-01	-4,08948E+02	1,88586E+04	-4,01632E+05	4,72019E+06	-3,29527E+07	1,40149E+08	-3,56792E+08	5,00400E+08	-2,97737E+08

2.2. Thermodynamic Model

The thermodynamic model implemented in this study distinguishes itself between the open phase and the closed phase of the internal combustion engine cycle. It is adopted a specific thermodynamic model for each phase, although both are based on the first law of thermodynamics.

2.2.1. Closed Phase

The closed phase of the engine cycle comprises the compression, combustion and expansion processes. The thermodynamic formulation for this phase is the first law of thermodynamics for a closed system, which is represented by Eq. (36) in the case of the variation effects of the kinetic and potential energy could be assumed negligible.

$$dU = \delta Q - \delta W \qquad (36)$$

The first term in the Eq. (36) is related to the variation of the internal energy of the gases inside cylinder dU, which is expressed by Eq. (37)

$$dU = dU_{products} * X_w(\theta) + dU_{reagents} * [1 - X_w(\theta)] + dU_{residual\,gas} \qquad (37)$$

, where $X_w(\theta)$ known as Wiebe function is given by Eq. (30).
The second term in the first law equation for a closed system δQ can be interpreted as Eq. (38)

$$\delta Q = dQ_c + \delta Q_p \qquad (38)$$

, where dQ_c represents the energy provided by burning fuel and δQ_p represents the instantaneous heat transfer with the cylinder walls, which is given by equation (26). The heat transfer coefficient for this phase is given by Eq. (27). The amount of energy supplied instantaneously by the fuel from its burning dQ_c is obtained by Eq. (39)

$$Q_c = \eta_c * m_c * PCI \qquad (39)$$

, where η_c is the combustion efficiency coefficient, m_c is the fuel mass admitted by the engine and *PCI* is the lower heating value of the fuel. The combustion efficiency η_c is obtained by Eq. (40), according to Alla (2002).

$$\eta_c = \eta_{max} * \left(-1,6082 + 4,6509 * \lambda - 2,0764 * \lambda^2\right) \qquad (40)$$

The maximum combustion efficiency η_{max} is around 90% for the conventional spark ignition engines according to Heywood (1988). Thus, the energy supplied instantaneously by the fuel in the interval $d\theta$ is given by Eq. (41).

$$dQ_c = \eta_c * m_c * PCI * [X_w(\theta_2) - X_w(\theta_1)] \tag{41}$$

Finally, the third term in the Eq. (36) is given by Eq. (42)

$$\delta W = \left(\frac{P_2 + P_1}{2}\right) * (V_2 - V_1) \tag{42}$$

, where P_2 and V_2 are the instantaneous pressure and volume in the current step of the algorithm while P_1 and V_1 are the instantaneous pressure and volume in the previous step, thus related to the angular interval $d\theta$.

2.2.2. Open Phase

The open phase of the engine cycle comprises the intake and exhaust processes. The thermodynamic formulation for this phase is the first law of thermodynamics for an open system, which is represented by Eq. (43) in the case of the variation effects of the kinetic and potential energy could be assumed negligible.

$$dU = \delta Q - \delta W + \sum_{vv} dm_e * h_e - \sum_{vv} dm_s * h_s \tag{43}$$

, where dm_e and dm_s are the masses going in and going out of the cylinder respectively and h_e and h_s are the enthalpies associated. The summation shown in the Eq. (43) refers to the sum of the energy flow through the vv valves in the engine.

The calculation of the variation in internal energy dU is analogous to the closed phase. The difference lies in the fact that at the open phase there are mass flowing between the cylinder and collectors and, therefore, it is necessary to know the composition of the mixture inside the cylinder at every moment.

The calculation of the heat transfer with the cylinder walls δQ in the open phase is similar to the closed phase and given by Eq. (38), with a distinction related to the heat transfer coefficient applied. The heat transfer coefficients for this phase are given by Eq. (28) and Eq. (29).

The procedure for calculating the work δW is identical to the closed phase and given by Eq. (42).

Thus, the last two terms of Eq. (43), which represent the energy flow through a control volume, could be calculated from the mass dm by Eq. (32) or Eq. (33) and its respective enthalpies h.

2.3. Block Diagram of the Computational Simulation Model

Once defined the theoretical fundamentals and the thermodynamic model, it is presented the algorithm programmed in MATLAB, which followed the block diagram shown in Fig. 4.

2.3.1. Input Data

The input data required for the simulation are mainly related to the ambient conditions, to the dimensional project, to the engine operating regime, to the fuel properties and to the substances involved in the process.

2.3.2. Preliminary Calculation

The main calculations performed in this stage are those related to the engine geometry equations (item 2.1.1.) and related to the balancing combustion reaction (item 2.1.2.).

2.3.3. Closed Phase

In the closed phase there is an inequality to be respected by the algorithm, which is based on the first law of thermodynamics for a closed system. Therefore, the calculations related to the variation of internal energy dU by Eq. (37), to the instantaneous heat transfer δQ by Eq. (38) and to the work δW by Eq. (42) are made for a specific crankshaft angle, at a given pressure and temperature and then it is verified if the inequality given by Eq. (44) is achieved

$$|dU - \delta Q + \delta W| < \chi \tag{44}$$

, where χ is the permissible error in the inequality. In this paper, it is admitted χ=0,001.

In the case this inequality do not be established, it is assumed a new temperature, it is calculated a new pressure by the equation of state, it is calculated again the terms of the first law and then it is again verified if the inequality is achieved. This calculation procedure is repeated until the condition is satisfied for the respective crankshaft angle. Then, it is incremented a step $d\theta$ in the simulation until it runs all the extension of the closed phase.
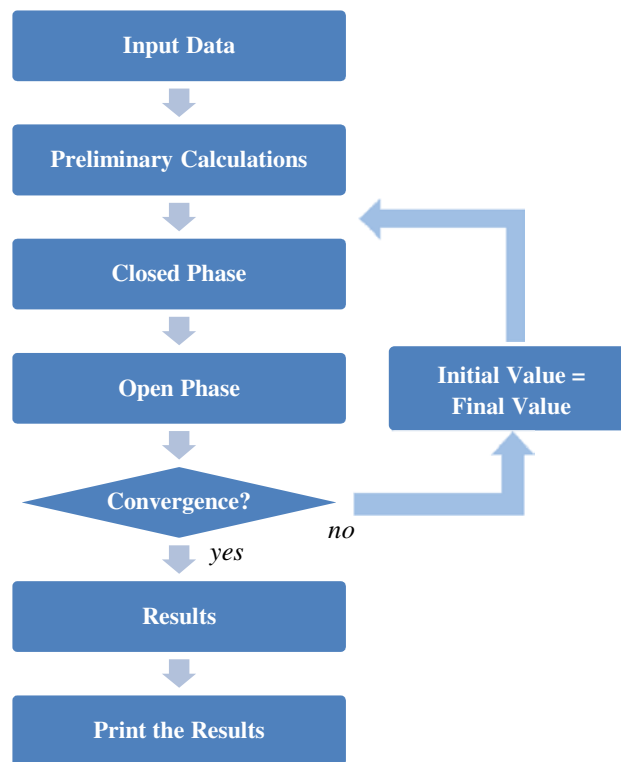
Figure 4 – The block diagram of the computational simulation model.

2.3.4. Open Phase

In the open phase there is an inequality to be respected by the algorithm, which is based on the first law of thermodynamics for an open system. Therefore, the calculations related to the variation of internal energy dU by Eq. (37), to the instantaneous heat transfer δQ by Eq. (38), to the work δW by Eq. (42) and the energy flow through the control volume are made for a specific crankshaft angle, at a given pressure and temperature and then it is verified if the inequality given by Eq. (45) is achieved

$$|dU - \delta Q + \delta W - \sum_{vv} dm_e * h_e - \sum_{vv} dm_s * h_s| < \chi \tag{45}$$

, where χ is the permissible error in the inequality, which is admitted the same of the closed phase.

Before proceeding to the next step of the simulation, it is recalculated the mass inside of the cylinder since there was a mass flow through the control volume at this angular interval $d\theta$. Then, it is incremented a step $d\theta$ in the simulation until it reaches the end of the open phase.

2.3.5. Convergence Verification

It was applied an inequality in the algorithm in order to establish its convergence, which is related to the difference between the calculated f_2 and the estimated f_1 values to the residual gas fraction of the engine. The inequality of the algorithm convergence is given by Eq. (46)

$$|f_2 - f_1| < \chi \tag{46}$$

, where χ is the permissible error in the inequality, which is admitted the same of the closed phase.

If this convergence criterion is not satisfied, the algorithm assumes the calculated data as best estimates for some initial trial data used in the simulation and then performs it again, since it is an iterative process.

2.3.6. Results

With the data obtained during the simulation of a complete engine cycle the algorithm perform some calculations and obtain all necessary results.

2.3.7. Print the Results

The results found are plotted for future analysis and then the simulation is finished.

3. MODEL EVALUATION

The computational simulation model has not been validated yet because it requires experimental results that shall be done soon. However, the input data applied in the simulation presented in this article are the same applied in the simulation performed by Gallo (1990), which are reported in Tab. 3. This procedure allows us to evaluate the consistency of the results obtained from the simulation model developed with the results found in literature.

Table 3 – Input data for the simulation (Gallo, 1990).

Ambient pressure (P_0)	101325	N/m²
Ambient temperature (T_0)	298,15	K
Displaced volume (V_c)	1598	cm³
Number of cylinders	4	-
Stroke (L)	79,5	mm
Bore (d)	80	mm
Connecting rod (l)	128	mm
Compression ratio (I)	12:1	-
Number of valves	8	-
Intake valve size [diameter (d_{va}) / lift (e_{va})]	30,93 / 9,28	mm
Exhaust valve size [diameter (d_{ve}) / lift (e_{ve})]	28,27 / 8,48	mm
Angle duration of intake valve lift (α_a)	230	º
Angle duration of exhaust valve lift (α_e)	245	º
Crankshaft angle to the intake valve starts to open	700	º
Crankshaft angle to the exhaust valve starts to open	490	º
Engine speed (N)	5200	RPM
Intake manifold pressure (P_{adm})	86000	N/m²
Exhaust manifold pressure (P_{esc})	115000	N/m²
Cylinder wall temperature (T_p)	520	K
Ignition angle (θ_{ig})	340	º
Low heating value of anhydrous ethanol (PCI)	27,72	MJ/kg

As previously mentioned, the computational simulation model developed considers the combustion with finite duration, the instantaneous heat transfer with the cylinder walls and the intake and exhaust processes.

The consideration related to the combustion with finite duration was possible by the use of the Wiebe function, in which for a stoichiometric air/fuel mixture results a profile shown in Fig. 5. The Wiebe function parameters used in the simulation are $a=5$, $m=2$ and $\Delta\theta_c=60$. The Wiebe function parameter $a=5$ represents the combustion of almost 99.33% of the fuel mass admitted by the engine cycle.
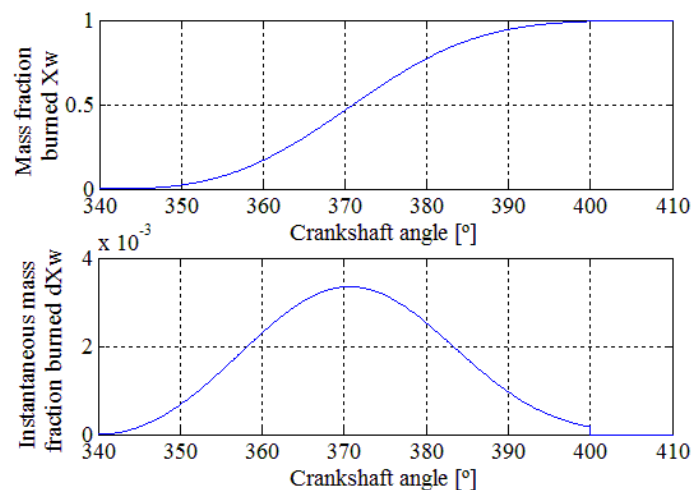

Figure 5 – The Wiebe function profiles as a function of crankshaft angle ($a=5$, $m=2$ and $\Delta\theta_c=60$).

In addition, a coefficient called combustion efficiency η_c was applied, proposed by Alla (2002), in the equation of the combustion process to take into account effects such as the thermal dissociation in the thermodynamic model, which occurs at high temperatures in real combustion processes. The amount of the combustion efficiency coefficient to a stoichiometric air/fuel mixture is η_c=0,87.

The consideration of the instantaneous heat transfer with the cylinder walls was made possible by the use of the equations proposed by Hohenberg (1979) and Nishiwaki (1979) to the heat transfer coefficient, whose profiles are shown in Fig. 6.
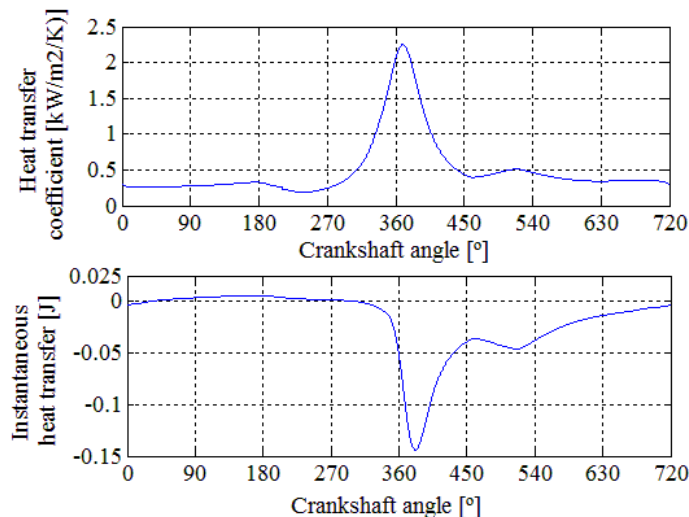

Figure 6 - The profiles of heat transfer coefficient and instantaneous heat transfer with the cylinder walls as a function of the crankshaft angle.

In Fig. 6 it is observed that in the most part of the engine cycle the gases are losing energy to the cylinder walls and the higher losses of energy happen during the combustion process, where there are higher temperature gradients.

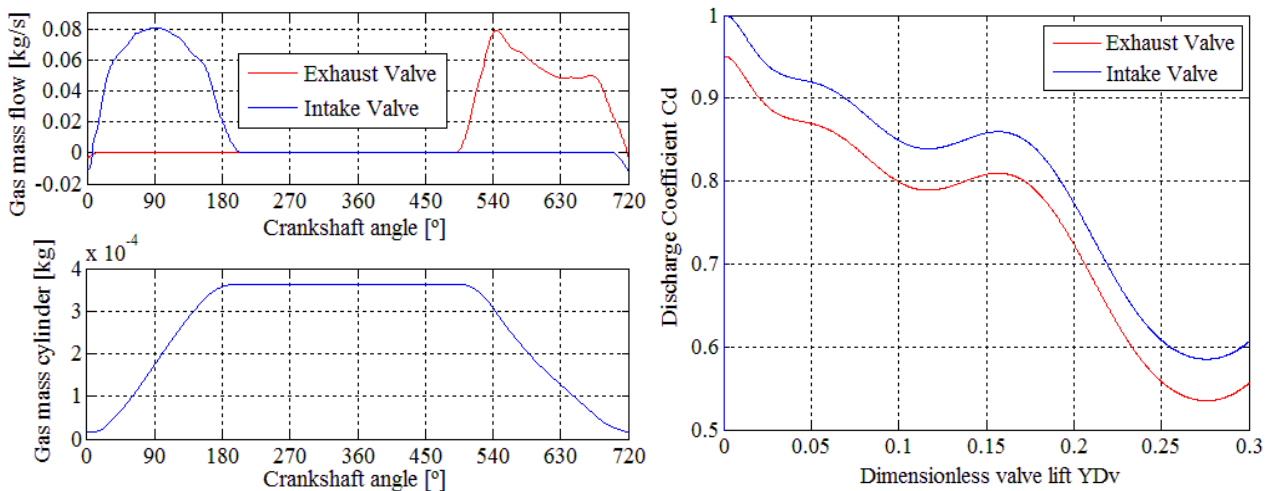The results related to the intake and exhaust processes are shown in Fig. 7.

Figure 7 – The profiles of gas mass flow through the valves as a function of the crankshaft angle and the profile of the discharge coefficient C_d as a function of dimensionless valve lift YD_v.

The mass flow of the gases through the intake and exhaust valves were represented in the first graph of Fig. 7. In it, there is a greater slope of the curve for the flow through the exhaust valve in the moments that follow its opening. This observation reveals the sonic flow in this period of engine cycle due to the high pressure gradients between gases inside of the cylinder and inside of the exhaust manifold.

Was observed in the second graph of Fig. 7 the amount of mass within the cylinder as a function of the crankshaft angle. Thus, it is possible to verify the amount of gas mass admitted into the cylinder during the closed phase of the engine cycle as well as the residual mass fraction that remains into the cylinder, which is related to the previous engine cycle.

After these considerations about the computational simulation model, the temperature and pressure profiles resulting from the simulation of an engine under operating at full load regime at 5200 RPM where presented below, whose input data are shown in Tab. 3.

In Fig. 8, it is presented the pressure and temperature profiles as a function of the crankshaft angle. In Fig. 9, it is shown the instantaneous pressure profile as a function of the instantaneous cylinder volume. The results obtained for the computational simulation model developed were compared to the results presented by Gallo (1990). Even with different models, it was verified that the results are quite similar. In the algorithm written by Gallo (1990) the chemical equilibrium and the gas dissociation are explicitly considered in the thermodynamic modeling while in the proposed model here these phenomena are addressed indirectly in the combustion equations through the combustion efficiency coefficient, proposed by Alla (2002).
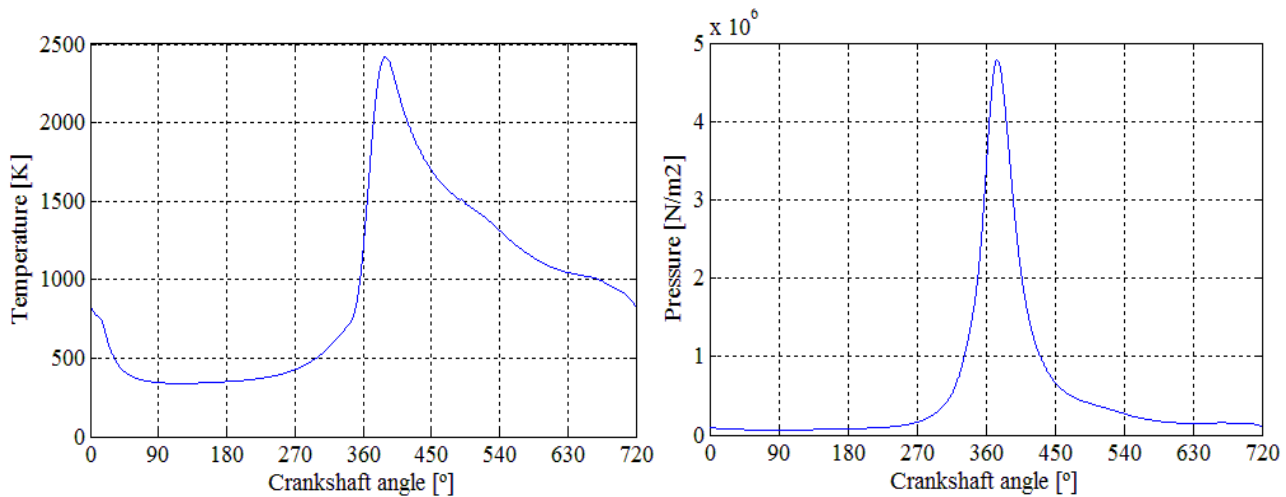
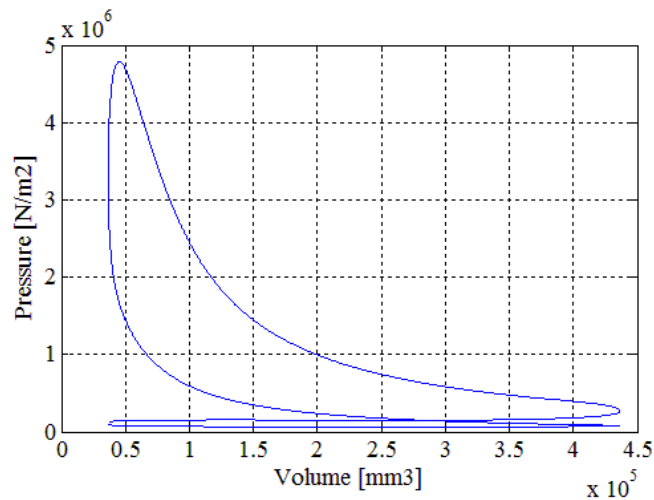Figure 8 – The temperature and pressure profiles as a function of the crankshaft angle.

Figure 9 – The instantaneous pressure as a function of the instantaneous cylinder volume.

4. SUMMARY

The computational simulation model developed showed to be very suitable to predict the temperature and pressure profiles obtaining similar results compared with the results found in literature. This result is very interesting since the developed algorithm uses thermodynamic and computational models less complex, moreover its editing and setup are simpler and the simulation time is greatly reduced.

Furthermore, from the computational simulation model developed it is possible to evaluate the influences of many engine parameters in the temperature and pressure profiles such as the engine speed, the load, the compression ratio, the ignition timing, the parameters related to the elevation of the valves, the stoichiometric ratio, etc.

It is worth mentioning that the computational simulation model developed by this study will become even more interesting after its experimental validation for a particular engine. It will allow the adjustment of certain constants used in some equations of the thermodynamic model. Thus, more reliable results could be obtained, making it a valuable tool in the development and testing of internal combustion engines.

5. ACKNOWLEDGEMENTS

6. REFERENCES

Alla, G.H.A., 2002. "Computer Simulation of a Four Stroke Spark Ignition Engine", *Energy Conversion and Management*, Vol. 43, n. 8 (May), p. 1043-1061.

Gallo, W.L.R., 1990. *Análise Exergética de Motores a Gasolina e Álcool*. Ph.D. thesis, University of Campinas, São Paulo, SP, Brazil.

Heywood, J.B., 1988. *Internal Combustion Engine Fundamentals*, McGraw-Hill, New York, USA, 1st edition.

Hohenberg, G., 1979. "Advanced Approaches for Heat Transfer Calculations". *SAE Transaction 790825*, p. 2788-2806.

Kastner, L.J., Willians, T.J. and White, J.B., 1963. "Poppet Inlet Valve Characteristics and Their Influence on the Induction Process". *Proc. Inst. Mech. Engrs. 178*, Part 1, nº 36, p. 955-978.

Nishiwaki, K., Shimamoto, Y. and Miyake, K., 1979. *Average Heat Transfer Coefficients on a Cylinder Wall in the Intake and Exhaust Processes of Motoring Test*. Bull JSME 22 (174), p. 1796-1809.

Raznjevic, K., 1970. *Tables et Diagrammes Thermodynamiques*. Paris Editions Eyrolles.

Sherman, R.H. and Blunberg, P.N., 1977. "The Influence of Induction and Exhaust Processes on Emissions and Fuel Consumption in the Spark Ignited Engine". *SAE Transaction 770880*, p. 3025-3040.

Stull, D.R. and Prophet, H., 1971. *JANAF Thermochemical Tables*. National Standard Reference Data System NSRDS-NBS-37, 2nd edition.

Zacharias, F., 1967. "Analytical Representation of the Thermodynamic Properties of Combustion Gases". *SAE Paper 670930*, p. 1-16.

7. RESPONSIBILITY NOTICE

The authors are the only responsible for the printed material included in this paper.